CHAPTER 7

CONVECTION FROM HEATED SURFACES

The problems which arise when the buoyancy sources are distributed over a surface, rather than being localized, are rather different from those treated in the previous chapter. Often the temperature difference between the fluid and the surface or between two surfaces is now specified, and the heat flux is not given but is a derived quantity which it is desired to predict. Attention is shifted from the individual elements to the properties of the mean flow and buoyancy fields, since it is not clear at the outset what form the buoyant motions will take. As we shall see later in this chapter, however, the details of the observed flows can only be properly understood if we again consider the buoyant elements explicitly and try to understand how their form and scale is determined by the boundary conditions (which in many cases are nominally uniform over the solid surface).

There is also the new feature of stability to be discussed here. A point source of buoyancy in an otherwise unconstrained perfect fluid always gives rise to convective motions above or below it, with an associated production of vorticity, and the same is true of a horizontal interface with the lighter fluid below (see § 1.2). In a real fluid, however, the criterion based on (1.2.1) is no longer sufficient to determine whether a horizontal layer of fluid is gravitationally unstable or not; even when the fluid is lighter below, molecular viscosity and diffusion can act to damp out small disturbances, so that no overturning occurs.

We begin with a discussion of the linear stability problem for convection between horizontal planes, proceeding straight to the case where both viscosity and diffusion are important, and go on to discuss theories describing this process when the amplitude is finite. The related experimental evidence will then be presented, together with the results of numerical experiments which complement the

laboratory results. The nature of the individual convective elements, and the way in which they interact with, and in some cases determine, the mean properties of their environment will be discussed next. Finally, a few problems relating to convection in different geometries will be presented briefly.

7.1. The theory of convection between horizontal plates

7.1.1. *The governing parameters*

The classic problem of thermal convection is to determine the motion of a layer of fluid contained between horizontal planes, uniformly heated below and cooled above. This continues to attract a great deal of attention, both because of its relation to the heat transfer at the earth's surface and the resemblance between convection patterns observed in thin sheets of cloud and in the laboratory, and because of its inherent mathematical and experimental interest to successive generations of workers in this field. This interest dates back to the experiments of Bénard (1901), who showed that a thin layer of fluid becomes unstable when the temperature difference exceeds a minimum value (which depends strongly on the depth and less strongly on the properties of the fluid). As discussed in more detail in §7.2, the motion at first takes place in a regular steady pattern, but with larger depths and temperature differences it can become turbulent. The meaning of the major parameter determining the behaviour can be appreciated by considering the following simple mechanistic model of the convection process (which is of course equivalent to a scale analysis of the governing equations).

Suppose that a small laminar buoyant element, with fixed characteristic dimension δ, leaves the neighbourhood of one boundary with density difference ρ_0' from the surrounding fluid, and that it subsequently has a density difference $\rho'(t)$. (In terms of temperature, $\rho_0'/\rho \approx \frac{1}{2}\alpha\Delta T$, where α is the coefficient of expansion and ΔT the temperature difference between the plates.) It is driven upwards (in the z-direction) by buoyancy forces but retarded by viscosity, and neglecting inertia effects there is the local balance

$$g\rho'\delta^3 \sim \mu\delta w \sim \mu\delta\frac{\mathrm{d}z}{\mathrm{d}t}. \tag{7.1.1}$$

Because of diffusion, the density difference ρ' will be decreasing from its initial value at a rate which depends on the surface area and is approximately

$$\frac{\mathrm{d}\rho'}{\mathrm{d}t} \sim -\frac{\kappa\rho'}{\delta^2}, \tag{7.1.2}$$

where κ is the thermometric conductivity, so that

$$\rho' \sim \rho_0' \exp(-\kappa t/\delta^2).$$

Combining (7.1.1) and (7.1.2) gives the total distance travelled between $t = 0$ and $t = \infty$ as

$$z = \frac{g'\delta^4}{\kappa\nu}. \tag{7.1.3}$$

If convection is to transport heat to a second plane a distance d from the first, the right-hand side of (7.1.3) must be greater than d. For fixed ρ_0', κ and ν conditions are most favourable when δ is as large as possible, i.e. is of order d, so marginal stability corresponds to a particular value of the parameter

$$Ra = \frac{g'd^3}{\kappa\nu} = \frac{g\alpha\Delta T d^3}{\kappa\nu}, \tag{7.1.4}$$

called the Rayleigh number.

The Rayleigh number remains the most important parameter over the whole range of more unstable conditions. As is clear from the above model, it expresses the balance between the driving buoyancy forces and the two diffusive processes which retard the motion and tend to stabilize it. Another interpretation following from (7.1.1) is that

$$Ra = w\delta/\kappa = Pe, \tag{7.1.5}$$

i.e. a Péclet number based on the parameters of the laminar motion set up by the buoyancy forces. The second parameter needed to describe the state of the fluid completely (for all problems except the initial instability) is the Prandtl number $Pr = \nu/\kappa$. The combination $Ra/Pr = Gr$ is the Grashof number, which arises (as in §4.2.3) in problems where the density difference is given and diffusion need not be taken explicitly into account. (See also §7.4.) The Nusselt number Nu, a non-dimensional heat flux, is defined as the ratio of the actual heat (or more generally, buoyancy) transport to the purely diffusive flux which would occur through a linear temperature gradient between the two boundaries, and it must be a function of

Ra and *Pr*. The Richardson number cannot enter here, because there is no externally imposed velocity, independent of the buoyancy forces.

7.1.2. *Linear stability theory*

A more detailed discussion of the methods used will be given in chapter 8, in the context of two-component convection; but the main results of historical importance should at least be mentioned here. The stability problem was first formulated and solved by Lord Rayleigh (1916), for the idealized case of free conducting boundaries with a linear temperature gradient. He used a perturbation expansion of the linearized Boussinesq equations, assuming a convection pattern which varies sinusoidally in the horizontal (x and y) directions (i.e. 'cells' of rectangular planform), and showed that there is a critical value of Ra, the non-dimensional ratio now called after him, below which a fluid heated from below is stable to small disturbances. At a value of $Ra_c = \frac{27}{4}\pi^4 \approx 657$, cells which fill the gap between the boundaries become unstable in a steady mode. There will be disturbances growing monotonically (in fact to a steady state, see §7.1.3) when $Ra > Ra_c$; at successively higher values of Ra other modes can appear. The Prandtl number ν/κ does not enter into this time-independent problem (cf. (7.2.2)). Jeffreys (1926, 1928) derived the differential equation for the small density perturbation ρ', whose eigenvalues determine the state of marginal stability (cf. (4.1.1)). In non-dimensional form this is

$$\nabla^6 \rho' = -Ra\left(\frac{\partial^2 \rho'}{\partial x^2} + \frac{\partial^2 \rho'}{\partial y^2}\right), \tag{7.1.6}$$

and an equation of the same kind follows for the velocity perturbation. Jeffreys again restricted himself to rectangular cells, but added the more realistic feature of rigid boundaries. He obtained solutions by numerical methods and showed that the most unstable two-dimensional cells (bounded by solid boundaries and by neighbouring upward and downward currents) are nearly square in cross section. The critical value of Ra (corrected by later work) is 1708, and with one rigid and one free boundary it is 1108; the constraining effect of rigid boundaries clearly makes the flow more stable. Jeffreys (1928) also pointed out that the presence of a small shear

will promote the stability of all modes except the two-dimensional one for which the cell boundaries are aligned in the direction of the shear. This in agreement with laboratory observations and with the recent detailed calculation of Gage and Reid (1968) for plane Poiseuille flow, to which reference has already been made in §4.2.2.

Pellew and Southwell (1940) relaxed the assumption of rectangular cells, and treated also circular, triangular and hexagonal boundaries. They showed that the horizontal and vertical variables in (7.1.6) can be separated by writing $\rho' = F(z)f(x,y)$, say, to give

$$[(\mathrm{D}^2 - a^2)^3 + a^2 Ra]F = 0 \qquad (7.1.7)$$

and

$$\frac{\partial^2 f}{\partial x^2} + \frac{\partial^2 f}{\partial y^2} + a^2 f = 0, \qquad (7.1.8)$$

where $\mathrm{D} \equiv \partial/\partial\zeta$, $\zeta = z/d$ and x and y are non-dimensional horizontal coordinates (also scaled with the depth of the fluid d). The number a^2 is a characteristic number of the horizontal structure, related to the cell shape; for rectangular cells with wavenumbers l and m it is $a^2 = (l^2 + m^2)d^2$.

The value of Ra corresponding to marginal stability is again found from the eigenvalues of (7.1.7), subject to the appropriate boundary conditions. In the case of rigid boundaries, the minimum value of Ra for the first mode in the vertical is represented as a function of a by the lower line in fig. 7.1. The minimum value for *any* a is the critical Ra_c, and this occurs at $a = 3.13$ compared with $a = \pi/\sqrt{2} = 2.22$ for two free boundaries. Note that this result is obtained without specifying the horizontal form of the cell, and indeed linear theory gives no information about the most unstable form. When a shape is specified, however, the most unstable size follows and the corresponding eigenfunctions of (7.1.8) give the initial form of the density distribution (and of the motion) satisfying the given boundary conditions. Exact solutions have been found for hexagonal and for annular cells, both for the case of two free boundaries.

7.1.3. *Finite amplitude convection*

The state of knowledge of the linear theory is now virtually complete (see Chandrasekhar 1961) and recent interest has concentrated on

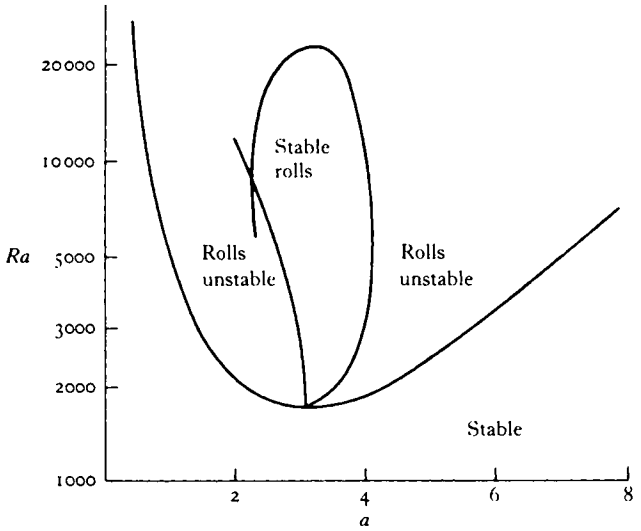

Fig. 7.1. Stability diagram for convection between rigid horizontal planes: the Rayleigh number plotted against horizontal wavenumber, showing the critical value for the first instability, and the region where two-dimensional rolls are stable according to Busse (1967).

the non-linear problems, associated with convection at higher Rayleigh numbers.

To obtain information about the steady amplitude and preferred planform of the finite motions established above Ra_c, one must take into account the advection of buoyancy and momentum by the flow field generated by the buoyancy, and therefore by definition must use the non-linear equations of motion. Malkus and Veronis (1958) showed, however, that the non-linear equations can be expanded as a sequence of linear equations whose solutions follow from those of the linear problem, and can thus again be found for any planform. Their perturbation method is based on an expansion parameter which is effectively $(Ra/Ra_c - 1)^{\frac{1}{2}}$, so it is valid only for relatively small departures from marginal stability. They suggested that the relevant solution will be the one for which the mean-square temperature gradient is a maximum, and on this basis predicted that square cells are preferred just above Ra_c in ordinary fluids. (There is no firm physical basis for this particular assumption, but some extra condition must always be used to close the problem when the boundary conditions at the sides are left unspecified.) The initial

heat flux due to convection depends nearly linearly on Ra on their model, up to $Ra = 10\,Ra_c$, and the preferred horizontal wavenumber increases with increasing Ra.

Schlüter, Lortz and Busse (1965) extended this expansion technique to investigate the stability of each of the possible steady finite amplitude solutions. They showed for both rigid and free boundaries that all three-dimensional cellular patterns in a fluid with fixed properties can be unstable with respect to infinitesimal disturbances. There is a range of parameters for which only two-dimensional rolls, having a more restricted range of wavelengths than suggested by the linear theory, are stable, and the boundary of this region (determined by Busse (1967) with the assumption of infinite Pr) is shown in fig. 7.1. Analyses in which the fluid properties are allowed to be functions of temperature, thus permitting some vertical assymmetry in the layer, suggest on the other hand that the hexagonal pattern can be stable just above Ra_c.

The application of these and related theories is limited to a small range of Ra near Ra_c; numerical methods developed to extend such calculations to higher Ra will be described in §7.2. In the other limit of very large Ra, when the flow is certainly no longer steady, different arguments must be sought. Some predictions can be made on the basis of dimensional reasoning, whose validity of course depends on the underlying physical assumptions being satisfied. Let us now assume that the buoyancy flux depends on the conditions very near the boundaries and is independent of the plate separation d and of Pr. It follows from the definitions of Nu and Ra that

$$Nu = c\,Ra^{\frac{1}{3}}, \tag{7.1.9}$$

since this is the only form which removes the dependence on d. The constant c can still depend on the boundary conditions, however.

With the assumption that d is no longer relevant, the distinction between two parallel plates and a single horizontal surface disappears. In both cases, the relation (7.1.9) may be rewritten, using the definition of Ra, in the form

$$\alpha H/\rho C_p = 2^{\frac{4}{3}} c(g\kappa^2/\nu)^{\frac{1}{3}}(\alpha \Delta T_{\frac{1}{2}})^{\frac{4}{3}} = A(\alpha \Delta T)^{\frac{4}{3}}, \tag{7.1.10}$$

where $(\Delta T_{\frac{1}{2}})$ refers now either to the temperature difference between one plate and the far environment or to *half* the temperature dif-

ference between two plates. One might expect then that the similarity arguments of §5.1 could be used to find the distribution of density and the fluctuating quantities at a distance z above the lower plate; in the 'free convection' regime where the direct influence of molecular properties can be assumed negligible,

$$\mathrm{d}\rho/\mathrm{d}z \propto z^{-\frac{4}{3}},$$

which is the form derived on p. 134.

We have deferred until now, however, the point raised by Townsend (1962), which is especially relevant close to the heated plates in the laboratory experiments and in the atmosphere in the complete absence of a wind. In these circumstances the initial organization of the flow produced in the boundary layer (thickness z_b say) dominates the behaviour in the turbulent region outside; z_b must depend only on the buoyancy flux B and the conductivity κ and so must have the form

$$z_b \sim \kappa^{\frac{3}{4}} B^{-\frac{1}{4}}. \qquad (7.1.11)$$

Because of this second relevant lengthscale all we can say on purely dimensional grounds is that the non-dimensional heat flux H_* must be some function of z/z_b. To go further, one must turn to more detailed theoretical arguments. Using the results of Malkus (1954*b*), it appears that H_* is a *linear* function of z/z_b, corresponding to $\mathrm{d}\rho/\mathrm{d}z \propto z^{-2}$ (in agreement with the results of Townsend's (1959) experiments, to be described in §7.2).

The theory of Malkus mentioned above has had a strong influence on later work, but an adequate treatment of its rather complicated structure would take us too far afield here. We will just refer to a review of the subject by Howard (1964), and summarize some of the results which have been obtained for large Ra. In addition to the form of the mean gradient, Malkus calculated the r.m.s. temperature and velocity fluctuations and obtained a numerical estimate for the constant c in (7.1.9). This is in reasonable agreement with experiments at large Pr, but no dependence on Pr is predicted by the theory.

Kraichnan (1962) extended the similarity arguments to study this dependence on Pr explicitly. For large Pr he distinguished three regions of the flow; close to the boundary both molecular conduction and viscosity are dominant, somewhat further out molecular viscosity

remains important but heat is transported by convection, and at greater distances eddy processes control both transports. Using a 'mixing length' type of analysis (but paying special attention to numerical factors in order to make quantitative predictions), he showed that the temperature gradient in the fully turbulent region is proportional to $z^{-\frac{4}{3}}$, and in the intermediate region to z^{-2}. For the Nusselt number, Kraichnan predicted in the two limiting cases

$$Nu = 0.089 Ra^{\frac{1}{3}} \quad \text{at high} \quad Pr, \tag{7.1.12}$$

$$Nu = 0.17 (Pr \cdot Ra)^{\frac{1}{3}} \quad \text{at low} \quad Pr. \tag{7.1.13}$$

The second result is valid only when $(Pr \cdot Ra)^{\frac{1}{3}}$ is appreciably greater than 6; otherwise $Nu = 1$ and the transport is purely by conduction. Note that this form follows from the assumption that only the boundary layer flow is important, and that the power law is changed if interaction with larger eddies (and therefore a definite lengthscale) is taken into account.

Mention should also be made of the more recent theoretical work which seeks to put upper bounds on the heat flux as a function of Ra using variational methods. The bounds on the power law and the multiplying constant originally obtained by Howard (1963) were rather weak, but the addition of more physically realistic constraints on the possible motions greatly improves the estimates (Busse 1969.) The final limiting form at high Rayleigh number, with many horizontal wavenumbers taken into account, is again $Nu \propto Ra^{\frac{1}{3}}$, though with only one or a few wavenumbers the exponent is reduced and there is also a weak dependence on $\ln Ra$.

7.2. Laboratory and numerical experiments on parallel plate convection

More detailed predictions about convection between parallel plates at intermediate Rayleigh numbers have been made using high speed computing techniques to solve the coupled non-linear equations of motion and diffusion. Both because this work has been strongly influenced by the laboratory results, and because the numerical approach itself represents a kind of experimenting with the system to determine the relative importance of the various terms, it is convenient to group them together here.

7.2.1. *Observations of laminar convection*

Many laboratory studies have followed that of Bénard. Much of the early qualitative work was aimed at reproducing the regular patterns often observed in convective clouds; Phillips and Walker (1932), for example, showed that a wide variety of forms of cellular structure can be obtained by suitable variation of the rate of shear. Brunt (1952, p. 221) sought to relate such experiments to the atmospheric observations, replacing molecular conduction and viscosity by the joint effects of radiation and turbulence, but the analogy is far from exact and a detailed explanation of the patterns is still not available. The tendency for long lines of cloud to form with their axes aligned along the direction of the shear can, however, be explained in just the same way as in the laminar case: the downstream modes are the only ones not inhibited by the shear. An example of the last effect is shown in fig. 7.2 pl. XI; compare this with the clouds resulting from the K–H mechanism (fig. 4.14 pl. X) which are aligned across the shear.

Quantitative experiments were first reported by Schmidt and Milverton (1935), who confirmed the predicted value of the critical Rayleigh number, and heat transfer measurements were begun by Schmidt and Saunders (1938). We can refer again to Chandrasekhar (1961, ch. 2) for the history of this work, and concentrate here on describing some of the more recent developments.

Koschmieder (1967) carefully repeated Bénard's experiments in silicone oil, using various shapes of convection chamber with free and solid top boundaries, and showed that the initial cellular pattern to form when the bottom is gradually and uniformly heated is the two-dimensional roll. The orientation of these rolls depends, however, on the shape of the sidewall boundary, and in a circular chamber, for example, they appear as a series of concentric annular rings (fig. 7.3 pl. XVI). With a solid top boundary this initial configuration persists at larger temperature differences, but with air above, the ring pattern breaks down into hexagonal cells – very regular if the air above is still, and more nearly random if air motions are not suppressed. It seems most likely now that variations of surface tension with temperature are an essential element in these and Bénard's original experiments with a free surface

(Pearson 1958). The measured wavelengths are in good agreement with the predictions of theories such as that of Nield (1964) which take this effect as well as the density instability into account.

It is possible to set up cells of arbitrary shape and scale with non-uniform heating of the fluid layer, as demonstrated by Chen and Whitehead (1968) using temperature perturbations imposed with radiant heating. In the range $Ra_c < Ra < 2.5\,Ra_c$ which they covered, they showed that when the disturbance was removed, the convection pattern approached that predicted by linear theory. Foster (1969), on the other hand, showed in a numerical experiment that a different finite amplitude disturbance can persist in a range where another solution is most unstable.

Krishnamurti (1968) has devised an elegant optical method of examining the plan-form of convection in a chamber having solid metal top and bottom boundaries. She traversed a beam of light across one side of the chamber and photographed in the perpendicular direction in the horizontal plane to pick out the cross sections of cells marked with aluminium powder. She has shown that roll cells (again aligned by the boundaries) occur at Rayleigh numbers just above critical when the mean temperature of the layer is fixed (fig. 7.4 pl. XVI). However, hexagons can be realized (under conditions where the dependence of fluid properties on temperture must be small) when the mean temperature is increasing steadily (at a rate η), and the temperature profile is thus non-linear. This observation is in agreement with her theory based on an expansion in both η and the amplitude, which also shows that there is a finite amplitude instability at a lower value of the Rayleigh number than the usually accepted one. This gives rise to stable hexagons in which the direction of motion (left undetermined in the linear Boussinesq theory) depends on the sign of η, being downwards if η is positive. Both these further predictions were verified experimentally (with values of η corresponding to a change in temperature of only a couple of degrees per hour), and they go a long way towards explaining discrepancies in previous experiments which were not so carefully controlled, or in which temperature differences were produced by heating or cooling at only one boundary.

Tritton and Zarraga (1967) investigated the cellular convection patterns produced by the instability of a layer of fluid heated uni-

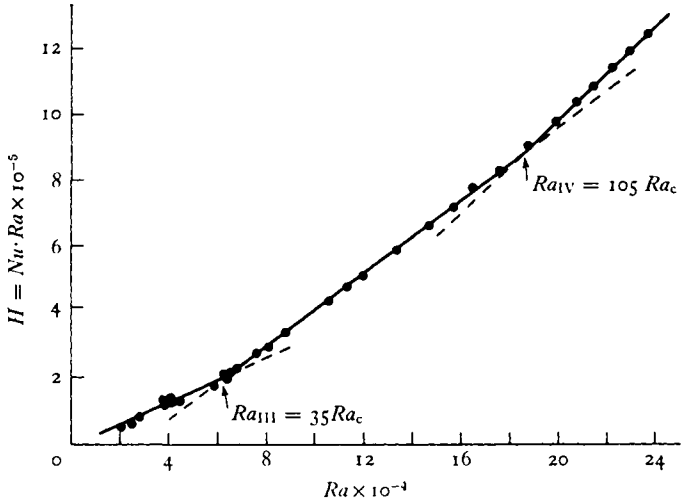

Fig. 7.6. Heat flux $H = Nu \cdot Ra$ as a function of Rayleigh number, showing the third and fourth transitions in a fluid with $Pr = 100$. (After Krishnamurti 1970.)

formly through its interior by an electrolytic current, and cooled from above. Hexagonal cells were formed in which the motion was downwards in the centre (in agreement with Krischnamurti's criterion), but more surprisingly the horizontal scale was much larger than with boundary heating. This observation becomes relevant when we wish to compare geophysical convection phenomena, especially in the earth's mantle, with laboratory results.

Heat flux measurements have been made by many experimenters, and the results are well summarized in a critical review by Rossby (1969). Recent experiments by Krishnamurti (1970), in which she has taken great care to study a series of steady states with fixed heat flux, have introduced a new order of precision into this field. She has shown that just above Ra_c the non-dimensional heat flux expressed as $H = Nu \cdot Ra$ is a linear function of Ra, with slope about 2.7 for water and slightly larger for fluids of higher Pr. At a second critical value Ra_{II} about $12\,Ra_c$ there is a discrete change to a higher slope, which was identified with a change in planform from two-dimensional to three-dimensional flow caused by a finite amplitude instability. Busse and Whitehead (1971) have also carried out experiments in this range, and have observed two distinct types of transition, which are shown in fig. 7.5 pl. XVII.

Further changes of slope in the heat flux curves at higher Ra are associated with transitions to time-dependent flows of various kinds (see fig. 7.6 and the next section). Malkus (1954*a*) had earlier obtained similar results (in unsteady experiments) but interpreted the transitions in terms of successive instabilities of higher order modes in the vertical.

7.2.2. *Measurements at larger Rayleigh numbers*

A feature of convection at high Rayleigh number, which has only recently become clear as experiments have been made in silicone oils of high viscosity and in liquid metals, is the strong dependence on Prandtl number. The transition to turbulence does not depend only on Ra reaching a value of order 10^5, as had previously been suggested; according to Rossby (1969) it occurs at $Ra \approx 14{,}000\, Pr^{\alpha}$, where $\alpha \approx 0.6$ for $Pr \gg 1$. When Pr is large, *steady* convection can persist to quite high Ra. The flux is then carried by large convection cells across which the velocity is gradually varying, but with temperature anomalies concentrated in narrow vertical regions at the cell boundaries which are fed directly by the boundary layer at the walls. As Ra is increased (for a given finite Pr) the motion becomes time dependent; remarkably regular oscillations are first observed, and these increase in number and frequency until finally the flow becomes more disordered and turbulent. The various regimes observed are shown in fig. 7.7 as a function of Ra and Pr. At small Pr, on the other hand (in mercury, for example, with $Pr = 0.025$), no steady flows are ever observed above Ra_c and flows at high Ra are always turbulent.

Various heat flux measurements show that some Prandtl number dependence persists even at large Pr and Ra (i.e. that the limit (7.1.12) is not approached in practice). Silveston (1958) and Globe and Dropkin (1969) respectively suggested the empirical relations

$$\left.\begin{aligned} Nu &= 0.10 Ra^{0.31} Pr^{0.05}, \\ Nu &= 0.069 Ra^{\frac{1}{3}} Pr^{0.074}, \end{aligned}\right\} \qquad (7.2.1)$$

to describe their experimental results for $Ra > 10^5$ and Pr from 0.02 to 8750. Rossby (1969) on the whole agrees with their individual measurements at the larger Pr, but questions the usefulness of

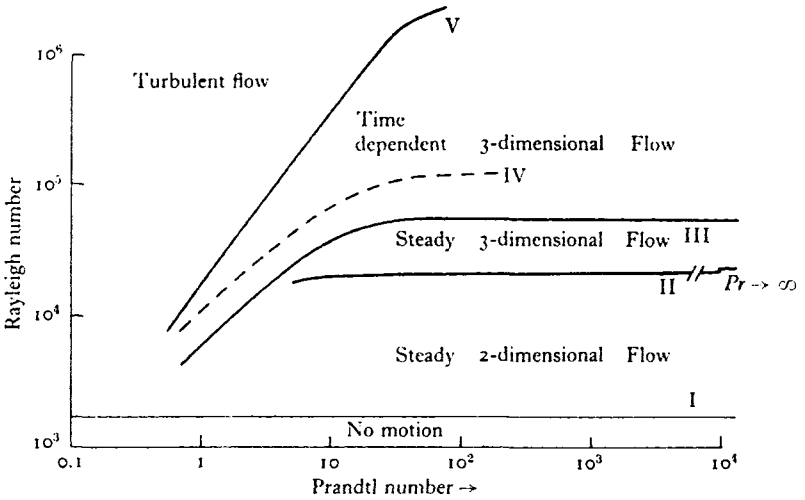

Fig. 7.7. Diagram showing the various forms of convection observed in a horizontal layer of fluid, as a function of Rayleigh and Prandtl numbers. (From Krishnamurti 1970.)

condensing all the results into a single formula, since as $Pr \to \infty$ the dependence on Pr should disappear. He also shows that the results for low Pr are quite different (cf. (7.1.13)). The power law dependence on Ra which he found using mercury, water and a silicone oil was consistently less than $\frac{1}{3}$, and the range of validity of this limiting value therefore remains in some doubt.

Thomas and Townsend (1957) and Townsend (1959) have made detailed measurements in air, recording mean and fluctuating quantities at various distances above a heated horizontal plate. Their measured heat fluxes imply a value of $C = 2^{\frac{1}{3}}c = 0.193$ in (7.1.10). (The corresponding value of c in (7.1.9), with Ra based on the whole temperature difference between two plates, is $c = 0.08$, slightly lower than the best value for water, $c = 0.09$.) Outside a purely conductive region, the mean temperature profiles were close to $T \propto z^{-1}$, the form predicted by the theory of Malkus (referred to in §7.1.3) which includes the direct effect of molecular diffusion near the wall. Their records of temperature fluctuations revealed periods of strong activity (which were more frequent close to the wall), alternating with relatively quiescent periods. These were interpreted as evidence for the intermittent detachment of buoyant elements

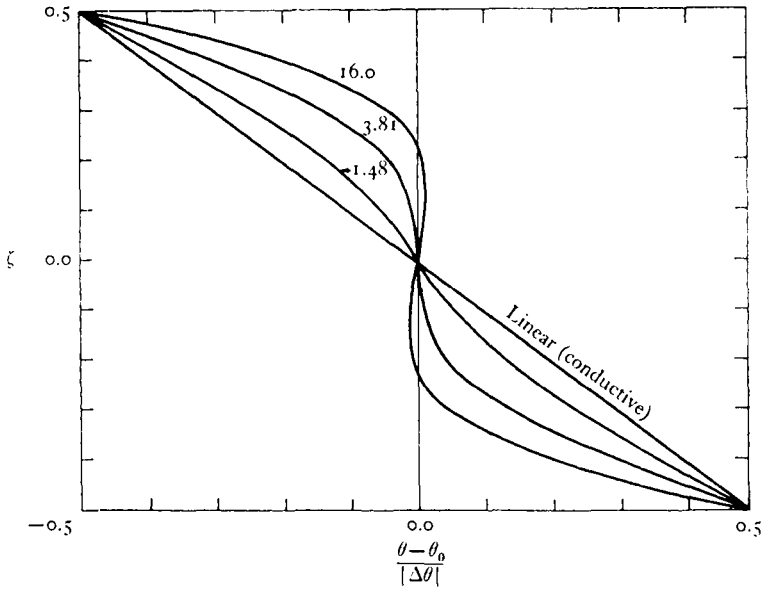

Fig. 7.8. Observed mean temperature profiles in a convecting fluid layer. (From Gille 1967.) Note the reversals of gradient at the larger values of $\lambda = Ra/Ra_c$, which are marked on the curves.

from the conductive boundary layer, and their subsequent erosion in the (still turbulent) surrounding air. Such observations point to the need to consider explicitly the nature of the buoyant elements and their interaction with the environment, which will be done in §7.3.

Other studies have concentrated on obtaining reliable mean profiles of the measured quantities, and comparing these with the numerical models. Deardorff and Willis (1965) compared the behaviour of a system constrained to convect in two-dimensional rolls with one in which three-dimensional, unsteady motions were permitted. In the latter case they showed that the heat flux was reduced by the unsteadiness and that averaging for a very long time is necessary before temporal and spatial estimates of the variance are the same; the former is crucially dependent on the slow shifting about of the convection pattern. In a later experiment (Deardorff and Willis 1967) they adopted the technique of spatial averaging and concluded that their observations were consistent with a thermal structure dominated by plumes extending most of the distance between the plates.

A feature of some of the detailed measurements, especially those at high Pr, is a reversal of the mean density profiles, which are slightly stable across the centre of the convecting region at high Rayleigh numbers. A particularly convincing experimental demonstration of this effect (in air with Ra about $16\,Ra_c$) was given by Gille (1967) using an optical method of measuring refractive index, which therefore did not require the insertion of any probes into the flow (fig. 7.8). This effect too can be explained (§7.3) in terms of the individual buoyant elements.

7.2.3. *Numerical experiments*

The predictions made using high speed computing techniques now far outweigh in detail those obtained from direct laboratory experiments, but only a few examples can be given here. They are all based on the numerical solution, with various approximations, of the coupled non-linear Boussinesq equations of motion and diffusion in two dimensions, which can be written in the non-dimensional form (Deardorff 1964)

$$\left(\frac{\partial}{\partial t}+u\frac{\partial}{\partial x}+w\frac{\partial}{\partial z}-Pr\nabla^2\right)\zeta = Pr\cdot Ra\frac{\partial T}{\partial x} \qquad (7.2.2)$$

and

$$\left(\frac{\partial}{\partial t}+u\frac{\partial}{\partial x}+w\frac{\partial}{\partial z}-\nabla^2\right)T = 0. \qquad (7.2.3)$$

Here $\zeta = \nabla^2\psi$ is the non-dimensional vorticity component in the y-direction, ψ is a streamfunction and T a non-dimensional temperature (proportional to the density).

Deardorff (1964) and Fromm (1965) retained the full form of the equations, and obtained solutions for just a few values of Pr and Ra. They imposed an initial disturbance on fluid at rest having an initially linear temperature gradient, and followed the development towards a steady state. The model is an essentially laminar one, leading at large times to the steady cellular convection pattern shown in fig. 7.9, which has the plume-like temperature structure characteristic of high Pr, high Ra convection (though the parameters used were $Pr = 0.71$ and $Ra = 6.75\times10^5$, corresponding to Townsend's experiments in air). A later model (Deardorff 1965) introduced extra assumptions to allow to some extent for three-

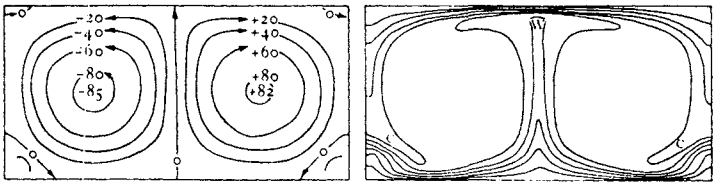

Fig. 7.9. Steady-state streamlines and isotherms calculated by Deardorff (1964) for a layer of fluid with $Pr = 0.71$, $Ra = 6.75 \times 10^5$. Relative values of the stream functions are given in the left-hand diagram; W denotes warm and C denotes cold regions in the right-hand diagram.

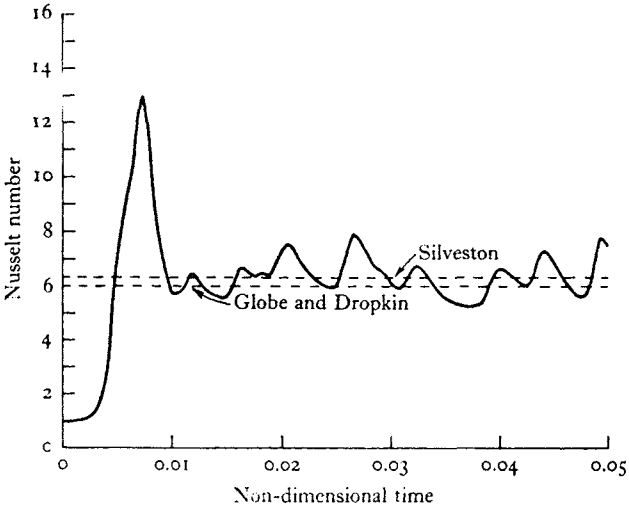

Fig. 7.10. The time-dependent heat flux calculated by Deardorff (1965), compared with laboratory measurements.

dimensional effects, and did permit fluctuations to persist. Fig. 7.10 shows the Nusselt number at $Pr = 0.71$, calculated by taking the horizontal average of the non-dimensional temperature gradient at the upper and lower boundaries. The computed mean heat flux was close to the measured values (also shown on the figure), and various other space-averaged quantities, such as mean density and the standard deviations of density and velocity were in rough agreement with observations. A wider range of steady conditions has been studied recently by Cabelli and de Vahl Davis (1971), who also included the effect of surface tension.

Herring (1963, 1964) introduced a model which greatly simplifies the analysis, and has also led to a clearer understanding of the important physical processes. His 'mean field equations' are obtained by averaging (7.2.2) and (7.2.3) over horizontal planes, retaining those non-linear terms which describe the interaction of the mean temperature field with a single velocity or temperature fluctuation, but omitting all interactions between fluctuating quantities. He was interested in the statistically steady state, and the limit $Pr = \infty$; a single, dominant wavenumber k was also assumed in the horizontal, which reduced the problem to one in a single space dimension (z). (Herring's calculations were based on a truncated Fourier representation of the variables in the vertical, but this should be regarded as a particular numerical technique, rather than an essential feature of the model.) For the case of rigid boundaries, the calculated heat fluxes at large Ra (corresponding to values of k chosen to maximize the heat flux in each case) were interpreted by fitting the form

$$Nu = 0.115 Ra^{\frac{1}{3}} \tag{7.2.4}$$

to the individual points. This is rather larger than the experimental values, and other functional relationships are not ruled out by his data; nevertheless the agreement between this (and other predictions of the model, such as the mean profiles) and the laboratory data are surprisingly good in view of the strong approximations made.

Elder (1969*a*) has shown that the mean field equations can be used to provide an adequate description not only of the steady state but of the temporal development of high Rayleigh number convection. He used an iterative finite difference method, with $Pr = 1$, and his paper contains an excellent discussion of the underlying assumptions, as well as a careful comparison with related work. At an intermediate stage of the calculation, a pronounced negative temperature gradient develops in the central region, and persists to the final state; this feature appears also (at the higher values of Ra) in all the numerical solutions described above. Observational evidence for such a reversal has been given in fig. 7.8, and the reasons for it will be discussed in the following section. Another feature of both Herring's and Elder's results is a small bump in the tempera-

ture profile at the edge of the unstable boundary layer. Though both of them attributed this to errors in their solutions, it may again represent a real physical effect (§7.3.4).

A finite amplitude solution for roll cells which retains the complete set of non-linear interactions has been obtained by Veronis (1966). For numerical reasons the number of terms must be truncated; but he has obtained in this way solutions valid for $Ra \lesssim 30Ra_c$ and over a range of Pr from 0.01 and 100. The stable solutions have the form of a single steady cell, which, however, accounts surprisingly well for the measured heat flux. A related model, which involves the expansion of the horizontal structure of all flow variables as a sum of solutions of the linear problem, has been proposed for high Ra and a general Pr by Gough, Spiegel and Toomre (1975). They average the resulting equations in the horizontal to obtain equations in z and t for the mean and fluctuating quantities. Retaining only the first terms in the series is equivalent to Herring's mean field approximation and leads as before to steady solutions. Including more terms, however, can produce *unsteady* solutions, some of which are periodic or aperiodic oscillations resembling those observed in Krishnamurti's laboratory experiments.

Information about turbulent convecting flows in a viscous fluid has also been obtained from numerical models designed primarily to study convection in a porous medium (Elder 1967). There is now the simplification that the dominant processes are the generation of vorticity by the horizontal gradient of the buoyancy forces (cf. (1.3.5) and (2.2.4)) and the transfer of heat by diffusion and advection, only the last being non-linear. By comparing such results with similar calculations which include the extra effects of diffusion and advection of vorticity (and again, from (7.2.2), only the former enters when Pr is large), Elder has determined how important these two processes can be; and in many cases the qualitative behaviour is little changed by them. We refer the reader to Elder's papers for a description of his numerical method, but will present some of his results in the context of the next section.

7.3. The interaction between convective elements and their environment

In the discussion of turbulent parallel-plate convection it has several times been remarked that certain properties of the mean distributions (of density for instance) can only be properly understood if one considers explicitly the behaviour of the buoyant elements themselves. In this section we therefore turn attention from the averaged distributions to the detailed observations, and the interpretation of these in terms of simple theoretical models. The ideas and terminology used have something in common with those of chapter 6, but the major difference here is that we can certainly no longer neglect the effect of the buoyant elements on the environment. On the contrary the distinction between the two is not clear-cut; the properties of the 'environment' are modified or even produced entirely by the convection elements, and there is a complex interaction between the two.

7.3.1. *The formation of plumes or thermals near a horizontal boundary*

Townsend's (1959) detailed observations, as well as common experience in the lower atmosphere, make it clear that the flux from a heated boundary is intermittent rather than steady. Buoyant fluid slowly accumulates and then breaks away, either as a thermal, or as an unsteady plume which wanders about the surface (unless there is some preferentially heated spot to which this can remain attached). All the theories presented so far fail to bring out this feature, but Howard (1964) has proposed the following model which considers it explicitly.

Suppose that a fluid layer of depth d is initially at rest and has a constant temperature $T = 0$. At time $t = 0$ the upper and lower boundaries have temperatures $-\frac{1}{2}\Delta T$ and $\frac{1}{2}\Delta T$ applied to them, and the fluid heats up by thermal conduction, producing error function profiles of the form

$$T = \tfrac{1}{2}\Delta T \operatorname{erfc}(z/2\sqrt{(\kappa t)}). \tag{7.3.1}$$

The thickness $\sqrt{(\pi\kappa t)}$ of the boundary layer increases, until at time t_*

the Rayleigh number Ra_δ based on ΔT and $\delta = \sqrt{(\pi\kappa t_*)}$ reaches a critical value, of order $Ra_\delta \sim 10^3$. At this time the buoyant fluid in the boundary layer suddenly breaks away as a discrete entity. With Pr of order unity and larger Howard has shown that this can happen in a time small compared with t_* (the model does not apply to low Pr, since conduction across the whole depth d will then be dominant). Thus for most of the time the process of transfer near the boundary is one of conduction, followed by a comparatively short interval during which the conditions are locally restored to the original uniform state by the removal of the buoyant fluid as a plume or thermal. Time averages of the conduction profile over the interval $(0, t_*)$ should therefore give estimates of the mean temperature profile and the heat flux which are equivalent to horizontal averages in the real flow. Howard's results, after averaging in this way, are

$$\bar{T} = \tfrac{1}{2}\Delta T[(1+2\xi^2)\operatorname{erfc}\xi - 2\pi^{-\frac{1}{2}}\xi e^{-\xi^2}] \tag{7.3.2}$$

with
$$Nu = d(\pi\kappa t_*)^{-\frac{1}{2}} = d/\delta = (Ra/Ra_\delta)^{\frac{1}{3}} \tag{7.3.3}$$

and
$$\xi = \tfrac{1}{2}z(\kappa t_*)^{-\frac{1}{2}} = \tfrac{1}{2}\pi^{\frac{1}{2}}z/\delta,$$

the other quantities being defined above. If t_* is determined by putting $Ra_\delta \approx 10^3$ then $Nu = 0.1\,Ra^{\frac{1}{3}}$, in reasonable agreement with experiment.

A comparison of this mean temperature profile with experiment is given in fig. 7.11. Townsend's (1959) measurements in air are shown and also some data in water obtained by Elder. Though only the shapes of the profiles are compared here, the results are consistent and the implied values of Ra_δ are reasonable. The r.m.s. temperature fluctuations at each level can also be calculated (considering only the conductive phase). This gives a profile having a peak in the boundary layer region of magnitude $(\overline{\theta^2})^{\frac{1}{2}} = 0.182\Delta T/2$, in remarkable agreement with Townsend's measured amplitude of 18 % of the temperature difference across the boundary layer, especially since nothing has been said about the contribution of the thermals themselves to $\overline{\theta^2}$.

This model has received strong support from the detailed laboratory and numerical experiments of Elder (1968). He has studied the flow both in a porous medium and a viscous fluid near a suddenly

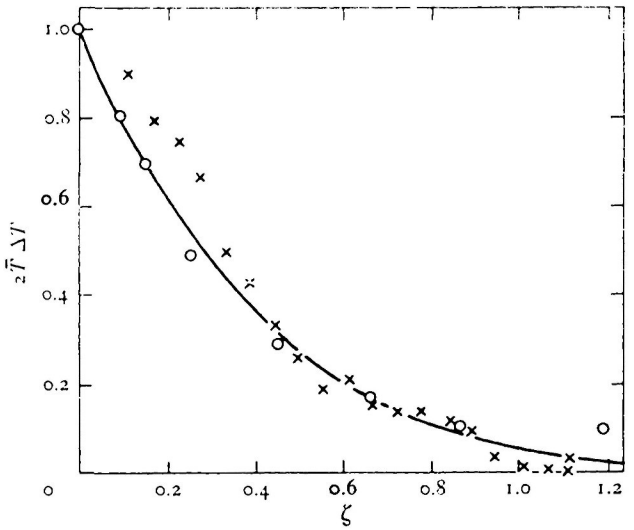

Fig. 7.11. Comparison of the mean temperature profile (7.3.2) with the experimental results of × Elder, ○ Townsend. (From Howard (1964), *Proc. 11th Congress Appl. Mech. Münich*, Springer-Verlag.)

heated horizontal boundary, and also (numerically) at an 'interface' or thin region of strong unstable temperature gradient separating two uniform layers. In all cases, when there is an initial source of temperature fluctuations, fairly regular cellular motions at first grow rapidly but remain confined within the boundary layer or interfacial region, with a horizontal scale which is of the same order as the interface thickness, and is unrelated to the total depth of the fluid. This simple but important result goes some way towards determining the scale and form of buoyant elements which was left entirely arbitrary in the calculations presented in chapter 6.

At later times, this layer becomes distorted and individual disturbances grow irregularly and break away from the boundary layer. These accelerate, even in the porous medium where inertial forces are by assumption negligible, because they can increase their buoyancy rapidly by entraining buoyant fluid from a surrounding volume. This happens before they lose their connection with the surface, and the process temporarily denudes a considerable area of the plate of its hot fluid, as shown clearly in fig. 7.12 where the stream function and isotherms are plotted at successive times for the special case of heating confined to a small area of the boundary.

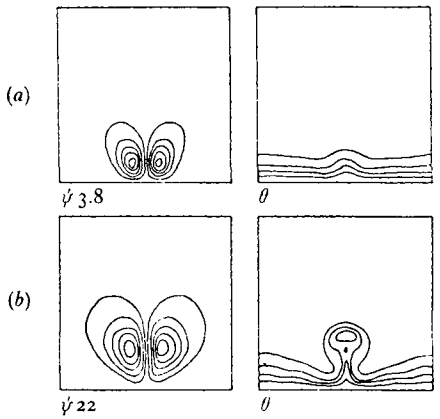

Fig. 7.12. Growth of a buoyant element near a heated section of the boundary, and its escape. Streamlines and isotherms calculated by Elder (1968).

Comparable (but of course less regular) patterns are obtained for the buoyant elements forming with random temperature fluctuations, and two photographs of a laboratory experiment of this kind are shown in fig. 7.13 pl. XVII. In similar experiments both Rossby (1969) and Sparrow, Husar and Goldstein (1970) observed a periodic formation and escape of thermals above preferred sites on the boundary, which they interpreted using Howard's ideas. (See fig. 7.14 pl. XVII.)

The time-dependent stability problem implied by this model has been studied by Foster (1965). He computed the time needed for an imposed disturbance to grow to specified multiples of its initial amplitude, and confirmed the importance of the conductive boundary layer thickness rather than the total depth. He showed that, except for very small heating or cooling rates, a quasi-steady calculation is misleading because the disturbances develop more slowly than the boundary layer itself. Foster has applied his theory to the interpretation of the onset of convection due to evaporative cooling of a free liquid surface. This occurs in the form of thin two-dimensional sheets plunging away from the surface, possibly because of the smaller constraint on the horizontal motion at a free surface compared to a solid wall. He has also shown (Foster 1971*b*) that it is possible to reproduce the intermittent character of the observations using a numerical model.

The extension of such 'initial instability' studies to fully turbulent convection of course requires further justification. The numerical calculations of Elder (1968) for the turbulent case do show the same features of formation and acceleration of thermals out of the sublayer with a characteristic size, though the details are affected by larger scale mean and turbulent motions. Considerable regularity of convection patterns is often observed in the atmosphere, as remarked in §7.2.1, but the prediction of the form and spacing of the convection elements as they leave the ground remains a major problem.

7.3.2. *The environment as an ensemble of convection elements*

Priestley (1959) has shown how one can obtain information about the mean properties and the fluctuations in the fluid over a heated plane by considering it as the superposition of many closely spaced convection elements having one of the special forms considered in chapter 6. As attention is shifted to the whole population instead of an individual plume or thermal, the process of entrainment is assumed to include the mixing of one element into another. First, the idea of the 'open parcel' (§6.4.4) can be extended to analyse the relative contributions to the heat flux of elements of different sizes. In a stable environment both very small and very large parcels are inefficient transporters of heat, the former because they are rapidly mixed, and the latter because their motion approaches a simple harmonic oscillation with w and ρ' a quarter cycle of phase. Imposed fluctuations in the form of parcels of an intermediate size produce the maximum buoyancy flux B_m, which can be written in terms of the variance of buoyancy fluctuations σ_ρ^2 and the (potential) density gradient as

$$B_m \approx \sigma_\rho^2 G^{-\frac{1}{2}} = \sigma_\rho^2 N^{-1} \qquad (7.3.4)$$

using the notation of §§5.2 and 6.4. This form is obtained immediately from a dimensional argument, given that B_m is to depend on σ_ρ^2 and G alone; the detailed mechanistic calculation only adds a numerical factor.

In the same way, if one interprets the results for the free convection regime (§5.1.3) in terms of a population of plumes, one must inevitably get the same form of dependence of the various quantities on height, though the multiplying constants depend on the particu-

lar model chosen. We have in fact already written down some relevant solutions in (6.4.2), for axisymmetric plumes with top hat profiles; specializing to $p = -\frac{4}{3}$ (appropriate for free convection) gives

$$w = C^{\frac{1}{2}}(\tfrac{3}{16})^{\frac{1}{2}}z^{\frac{1}{3}}, \quad g' = \tfrac{1}{2}Cz^{-\frac{1}{3}}, \quad b = \tfrac{6}{7}\alpha z. \tag{7.3.5}$$

The non-dimensional heat flux H_* for a single plume of this kind is by definition (5.1.14)

$$H_* = g'w/(Cz^{-\frac{1}{3}})^{\frac{3}{2}}z^2 = 0.22. \tag{7.3.6}$$

The important point here is that the argument gives a purely numerical constant characteristic of the plume, though as it happens the point source with top hat profile is a poor model of the atmospheric process, and more realistic results are obtained with line sources and Gaussian profiles. In comparing with the observed value of H_* in the atmosphere allowance must also be made for the fraction of the area convered by ascending plumes, which observation suggests is about $\frac{1}{2}$. (Priestley 1959, p. 88.)

7.3.3. *Convection from small sources in a confined region*

In this section we consider another kind of model which illuminates certain unsteady aspects of the problem of convection from sources near boundaries of a confined region. The type and spacing of the buoyancy sources will be regarded as given; the difficulties of specifying these for a uniformly heated surface have already been pointed out, but even a broad pattern of non-uniform heating will tend to organize the unstable regions into narrow plumes. (See Stommel 1962.) The convection elements are assumed to be far enough apart not to interact directly, which in practice means a separation greater than about twice the total depth. The environment will be assumed to be non-turbulent (though a more elaborate model which takes account of turbulence inside and outside rising plumes has been proposed by Telford (1970)). Thus the methods of chapter 6 can be used, but attention will now be focused on the properties of the environment rather than exclusively on the plumes or thermals themselves.

It is often clear in the laboratory that experiments on plumes can only be continued for a limited time before the walls of the containing vessel begin to affect the flow and the buoyant fluid modifies

the environment through which the plumes are moving. The same is true of the lower atmosphere; during the course of a day, the air below cloudbase heats up, due to the transfer of heat from the ground in the form of plumes or thermals. In this relatively deep layer the heat flux is decreasing with increasing height, not constant as was assumed in §5.1.3 for the layer very close to the ground. Eventually, in a region of limited extent, fluid which has been in the convection elements begins to 'fill up the box' and become part of the environment, and so changes in the latter become an integral part of the problem and cannot be ignored as they were in chapter 6. The effect is shown in fig. 7.15 pl. XVIII taken during an experiment in which a turbulent plume of salt solution was supplied at the top of a tank of fresh water for a long time. Dye put into the flow at an early stage spreads out along the floor, and this marked fluid thereafter becomes part of the environment, in which turbulence is quickly suppressed. A later marked patch of plume fluid passes through this slightly heavier layer and, as a result of mixing with it, becomes heavier still. The net result of this process is to produce a *stably stratified* environment, made up of fluid which has all passed through the plumes.

Baines and Turner (1969) have based a detailed theoretical model on this picture, using the entrainment equations (6.1.6) for plumes, but with $G = N^2$ now regarded as an unknown function of height. Assuming that the plume fluid spreads out instantaneously across the region at the top or bottom of the region (of height H, radius R) and becomes part of the non-turbulent environment at the same level, two extra equations can be written down linking G and the vertical velocity U in the environment. The first is just the continuity equation at any level which is

$$wb^2 = -UR^2 \tag{7.3.7}$$

(provided $b \ll R$). The second expresses the fact that the density of a particle in the non-turbulent environment remains constant, and that the only density changes at a fixed height occur because of the vertical motion:

$$\frac{\partial g_0}{\partial t} = -U\frac{\partial g_0}{\partial z} = UG, \tag{7.3.8}$$

where g_0 is the buoyancy parameter for the environment.

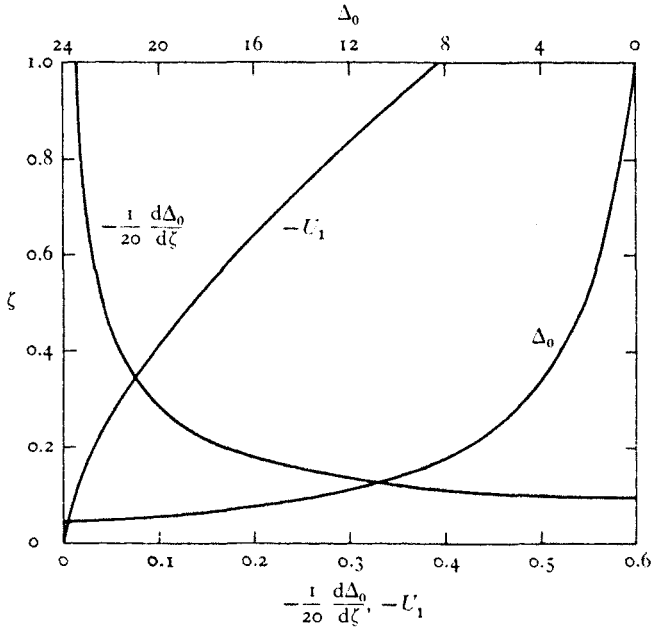

Fig. 7.16. The asymptotic properties of the environment, in non-dimensional form, produced by an axisymmetric plume in a closed region. U_1 is the vertical velocity of the environment, and $d\Delta_0/d\zeta$ is the density gradient.

The general problem is time dependent, but several special cases are more tractable. In the asymptotic state at large times t, only g_0 depends on t; the density of the environment changes linearly in time at all heights, while the *shape* of the density profile and all the other properties remain fixed. The equations can be reduced to non-dimensional form by scaling with H and the buoyancy flux F_0 at the source; for instance the environment is described by

$$\left.\begin{aligned} g_0 &= \tfrac{1}{4}(\pi)^{-\frac{2}{3}}\alpha^{-\frac{1}{3}}F_0^{\frac{2}{3}}H^{-\frac{5}{3}}[\Delta_0(\zeta)-\tau], \\ U &= 4\pi^{-\frac{1}{3}}\alpha^{\frac{1}{3}}F_0^{\frac{1}{3}}H^{-\frac{1}{3}}\left(\frac{H}{R}\right)^2 U_1(\zeta) \end{aligned}\right\} \qquad (7.3.9)$$

using subscripts to denote non-dimensional functions of $\zeta = z/H$. The width R enters only into the scaling of U and t; the distributions of density and the plume properties depend on H alone, but the time to achieve these does depend on R (i.e. on the spacing of the plumes).

The solutions for several of these non-dimensional functions are shown in fig. 7.16 (and essentially the same qualitative behaviour was obtained theoretically for two-dimensional plumes and axi-symmetric thermals). The form of the density distribution was checked experimentally in two ways, directly and by relating it to the motion of the dyed fluid layers, and these were both found to be in excellent quantitative agreement with the theory. The sharp stable density gradient in the environment near the source was clear in the experiments; it is not realistic for the atmospheric near the ground, but the theory can be modified to allow for a well mixed layer there. The slightly stable gradient at greater heights is, however, a feature of aircraft measurements below cloudbase (Warner and Telford 1967) even in conditions of strong convection, and it is a property which is preserved in the theoretical solutions even when horizontal averages are taken which include the plumes.

The relation of this calculation to the parallel plate convection problem now becomes clear. If buoyant elements emerging from one boundary layer can travel nearly to the opposite plate before losing their identity then this experiment can be thought of as a box filling up from both above and below with thermals (or unsteady plumes). (The picture is complicated, but not qualitatively changed, by the fact that the environment is turbulent.) This process can in time produce the slightly stable gradient in the interior which is observed, and also perhaps the more stable region at the edge of the unstable boundary layer which has been reported in the numerical experiments described in §7.2.3.

The model also explains in physical terms how there can be a 'counter-gradient' heat flux, which at one time caused a great deal of controversy (Priestley 1959, Deardorff 1966). Individual buoyant elements can clearly transport heat upwards in the atmosphere even though the mean temperature is greater at the top and the environment stably stratified. It is not helpful to interpret the transfer in terms of an eddy diffusivity when the motions are dominated by buoyancy, since the convective mechanism is not properly described by a relation between the flux and the local mean gradient.

7.3.4. *Penetrative convection*

The term 'penetrative convection' has come to mean the process whereby convective motions arising in an unstable region penetrate into an adjacent stable layer. It has also sometimes been used, logically enough, to distinguish the 'buoyant element' models treated in chapter 6 from the cellular motions observed at low Rayleigh number. When the convection is turbulent, this latter is no longer such a useful distinction to make, and so the first definition is used here. The problem is an important one for the lower atmosphere and upper ocean, where a layer of convecting fluid, driven by heat transfer across the surface, is bounded above (or below) by a stable gradient. As heating (cooling) is continued the depth of the convecting layer increases at the expense of the stable region, and so in general one must consider a time-dependent problem. Some of the properties of such systems, particularly the mixing across the fluid boundary, will be treated more fully in chapter 9.

An instructive laboratory model has been described by Deardorff, Willis and Lilly (1969). They set up a nearly linear stable temperature gradient in a tank of water, increased the temperature of the bottom to a new fixed value so that convection began, and measured vertical profiles of the horizontally averaged temperature as functions of time (fig. 7.17). (Note that the gradient becomes slightly stable below the top of the 'well-mixed' layer, suggesting that a 'filling box' model might be appropriate here too, with now a variable depth, instead of a fixed upper boundary.) Deardorff *et al.* deduced heat flux profiles, and showed that the upward flux decreases nearly linearly with depth above the bottom (as is to be expected for a layer of almost constant temperature). In a thin region at the top, however, the heat flux is downwards i.e. heat has been added to the convecting layer from the gradient region above. This latter effect is small, and the rate of rise of the interface can therefore be inferred pretty accurately by considering only the heat balance of the layer, equating the input to that necessary to heat a layer of increasing depth. A somewhat unrealistic feature of these experiments was that the temperature of the lower boundary was kept fixed, rather than the heat flux (a more natural boundary condition at the earth's surface). The flux can of course

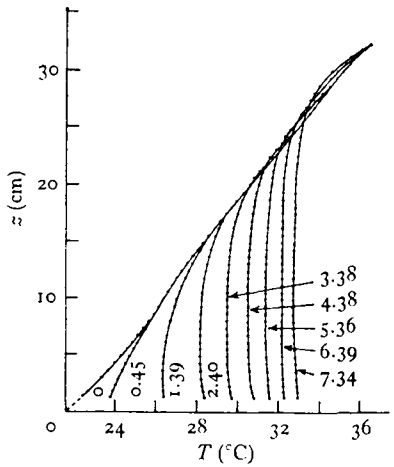

Fig. 7.17. Vertical profiles of temperature in a laboratory tank, set up initially with a linear stable temperature gradient and heated from below. The profile labels give the time in minutes. (From Deardorff, Willis and Lilly 1969.)

always be calculated from a relation of the form (7.1.10), but when it is assumed to be constant, especially simple relations can be derived for the depth and temperature of the convecting layer, which both increase like $t^{\frac{1}{3}}$. (See §8.2.1, where these are derived and compared with experiments, in the context of a *salinity* gradient heated uniformly from below.)

Another kind of experiment was reported by Townsend (1964) who made use of the non-linear density behaviour of water (which has its maximum density near 4 °C). He set up a tank of water with an ice-covered bottom and an upper surface at about 25 °C, so that the water at the bottom was convectively unstable while a stable gradient at the top was maintained by molecular conduction. After an establishment period (of about ten hours, starting with water at room temperature), during which the convecting layer grows in the manner described above, a steady state is attained which is very convenient for the detailed study of penetrative convection, both visually and by recording the fluctuations.

Townsend showed that vigorous overturning was confined to a thin region near the bottom, but that columns of fluid emerge from this, and penetrated through the whole 'convecting' layer, finally

being deflected horizontally as they reached the region of very stable stratification. The temperature of the mixed layer was nearly constant at 3.2 °C (below that of maximum density) but there was evidence of a slightly stable gradient, with more pronounced overshoots near the edges of this region. This again suggests the 'filling box' model (but without the location and spacing of the sources being specified), and it also gives some experimental support for the reality of the peaked form of profiles obtained numerically by Herring (1964) and Elder (1969*a*).

Temperature measurements in the ice–water system revealed the surprising feature that the fluctuations are a maximum just beyond the point of furthest penetration of the convective columns, in a thin region at the bottom of the stable layer. They are continuous rather than intermittent and so cannot be due to individual impacts of the 'columns', but they can be explained in terms of internal wave theory. In subsequent papers Townsend (1965, 1966, 1968) explored further the properties of waves produced by a convecting layer and also by a turbulent boundary layer generated by shear at the ground. He showed (as we should expect from §2.2) that when the duration of the impacts is long compared with N^{-1} the spread is predominantly horizontal, in agreement with his laboratory observations. He also suggested that the results can be applied to stratocumulus clouds, and that the 'clear air turbulence' observed just above and sometimes several kilometres to the side of convecting clouds is in fact a vigorous internal wave motion generated by the penetrative convection. The theory leads to numerical predictions which are consistent with this interpretation, provided the motions in clouds are persistent plumes rather than isolated thermals. (It is not yet clear from direct observation that this assumption is valid, and we mention in passing an alternative suggestion of Turner and Yang (1963). They regarded the region above a stratocumulus cloud as dynamically part of the turbulent cloud itself, which happens to be invisible because of evaporation following turbulent mixing with drier air above. A non-linear density behaviour was also included in their laboratory model of this process.)

Several numerical models of penetrative convection have been based directly on the ice–water convection experiments (though they have been applied to solar convection rather than geophysical

problems). Veronis (1963) used a series expansion method (a modification of that used earlier by Malkus and Veronis (1958)) to investigate the stability problem for a fluid in which the equation of state is parabolic, i.e.

$$\rho = \bar{\rho}[1 - \alpha(T - T_0)^2]. \tag{7.3.10}$$

His infinitesimal amplitude analysis showed that the value of a critical Rayleigh number (based on the thickness of the unstable layer, between 0 and 4 °C) is affected by the presence of stable fluid above 4 °C; the minimum Ra_c with the relaxed upper boundary condition is about one third of that in the ordinary Bénard problem and occurs when the temperature of the upper plate is about 6.7 °C. The second order terms indicated further that a finite amplitude instability can occur at an even smaller Rayleigh number, because any finite mixing motion which mixes two parcels of water with temperatures above and below 4 °C will create a layer of fluid near the maximum density, but deeper and therefore more unstable than the corresponding layer in a purely conductive state.

Subsequent stability calculations by Whitehead and Chen (1970) have modified Veronis' conclusion. They treated a variety of temperature profiles through a thin layer of unstable fluid bounded by a stable layer, and showed that, whereas a weak stable stratification reduces Ra_c, a very stable layer can remove energy from the unstable region and thus lead to an increase in the critical Rayleigh number above that for a solid boundary. They also produced comparable temperature distributions using radiant heating, and studied the stability and the subsequent supercritical motion, in which plunging vertical plumes were prominent (cf. §7.3.1).

Musman (1968) obtained steady-state finite amplitude solutions for the parabolic initial profile (7.3.10). He used the 'mean field' approximation of Herring (1963) (with one mode in the horizontal but many in the vertical), and compared his results with Townsend's (1964) measurements. The agreement through the convecting region is excellent (including a mean temperature less than 4 °C, and the stable gradient), but not so good in the conducting region above, where side wall heat fluxes were certainly important in the experiment. Musman showed that when the temperature of the upper boundary is about 7 °C or higher, convection first takes place

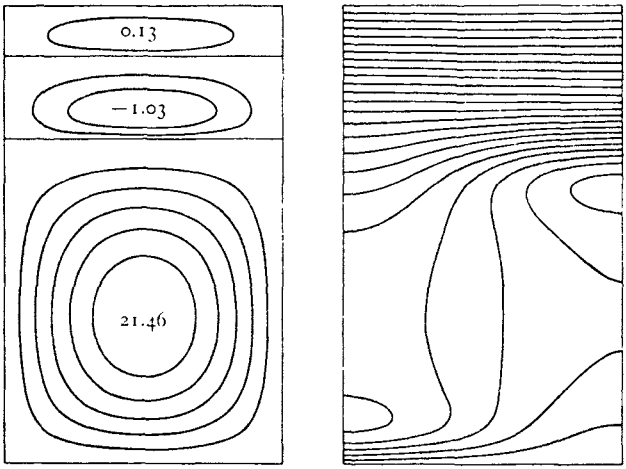

Fig. 7.18. Streamlines and isotherms calculated for 'convection over ice' by Musman (1968). The maximum vertical velocities in each cell are marked, and isotherms are plotted for each degree C from 0 at the bottom to 24 at the top.

at finite amplitude (in agreement with Veronis) and that when it is above 10 °C, the upper boundary is no longer dynamically important. The largest motions consist of a convecting cell extending from the lower boundary to the level where the temperature is 7 or 8 °C, with above this one or more counter cells, whose structure depends on the Rayleigh number. (See for example fig. 7.18.) The penetration of convection into the stable layer takes the form of nearly horizontal motions associated with the upper part of the main cell.

7.4. Convection with other shapes of boundary

We turn now more briefly to motions produced by buoyancy forces in different geometries, which have not been so intensively studied as the Bénard–Rayleigh problem, but which are nevertheless important in many applications.

Many of the flows of practical interest can be illustrated by considering a circular pipe of diameter d in various orientations. Suppose first that the axis of the pipe is vertical, that it is open above and below, and contains a fluid which is set into laminar motion because of a density difference between the fluid inside and outside the pipe.

Balancing the buoyancy force against the viscous stress at the walls shows that the velocity is $\overline{w} \sim g'd^2/\nu$ and the Reynolds number $\overline{w}d/\nu \sim g'd^3/\nu^2 \sim Gr$, justifying the statement made in §7.1.1. The Grashof number is the appropriate dimensionless parameter (and is equivalent to a Reynolds number) in convection problems where the density or temperature difference is *given*. The molecular diffusivity, and hence *Pr* or *Ra*, enters when the mechanism of heating the flow from the solid walls is of interest; when flows in a single fluid, and therefore at a fixed Prandtl number, are being compared the distinction is less important.

'Fully forced' convection, and heat transfer into a moving stream, will not be considered here (for an outline of the principles of this subject see, for example, Prandtl (1952), p. 397). One case of 'mixed' convection, the flow under a fixed pressure gradient in a long vertical heated pipe, will be described qualitatively. When the pressure gradient and buoyancy forces act together (i.e. the forced flow is upwards in a heated pipe), velocity and thermal boundary layers are formed, as they are when there is no pressure gradient. Provided the Rayleigh number (based on the pipe diameter and the change in temperature along the pipe in a length equal to the diameter) is sufficiently large, the upflow and heat flux are concentrated close to the wall, and there can be a slow reversed flow in the stably stratified fluid near the centre. On the other hand, if the pressure gradient and buoyancy forces are opposed, there will be a tendency for the whole motion to become unsteady and turbulent above a certain critical Rayleigh number, since the density distribution in the vertical will then be unstable. It will therefore be most effective, because of the convective motions which are induced, to heat fluid by passing it *down* a hot pipe. (cf. §6.2.3). Detailed similarity solutions exhibiting these features have been worked out by Morton (1960) for the special case of a pipe having a constant linear temperature gradient along it.

The phenomena observed in heated *horizontal* pipes, with or without an axial flow, are entirely different. Then there will be a circulation in the plane of the cross section, whose form depends on the distribution of heating and cooling and on the Rayleigh number; a problem of this kind is discussed in §7.4.3. The convective flow produced in the fluid *outside* a heated pipe (or horizontal cylinder) is

also of some importance. Near the body this can be treated by much the same methods as a vertical surface (§7.4.1), to determine the form of the boundary layer and the total heat flux into it with a given temperature difference. Far from the body, the flow detaches from the cylinder and becomes a plume whose properties can be expressed in terms of the height and the buoyancy flux, using the similarity arguments of chapter 6.

7.4.1. *A heated vertical wall*

The essential properties of free convection near a solid body can be brought out by considering a two-dimensional flow near a vertical boundary. Typically, this is held at a temperature T_1, different from that of the fluid (T_0) in which it is immersed, but the problem will be discussed here (as in §3.3.4) in terms of the local density difference ρ' set up between the fluid and the surroundings. Let ρ_1' denote the (fixed) density difference between fluid at the surface and at large distances from it, and $\gamma = \rho'/\rho_1'$.

When the convecting fluid is confined to a thin layer near the wall, the vertical equation of motion can be simplified to a boundary layer form, neglecting higher derivatives in the verticial (z) direction. This and the diffusion equation (cf. (3.3.15)) may be written

$$\left.\begin{aligned} u\frac{\partial w}{\partial x}+w\frac{\partial w}{\partial z} &= \nu\frac{\partial^2 w}{\partial x^2}+\frac{g\rho_1'}{\rho_0}\gamma, \\ u\frac{\partial \gamma}{\partial x}+w\frac{\partial \gamma}{\partial z} &= \kappa\frac{\partial^2 \gamma}{\partial x^2}, \end{aligned}\right\} \tag{7.4.1}$$

with boundary conditions $u = w = 0$, $\gamma = 1$ at $x = 0$, and $u = 0$, $\gamma = 0$ at $x = \infty$. Defining the stream function ψ in the usual way (§3.1.3) similarity solutions can be found for ψ and γ using the variable

$$\eta = \left(\frac{g\rho_1'}{\rho_0}\right)^{\frac{1}{2}}\nu^{-\frac{1}{2}}xz^{-\frac{1}{4}} = (Gr)^{\frac{1}{4}}\left(\frac{x}{H}\right)\left(\frac{z}{H}\right)^{-\frac{1}{4}}, \tag{7.4.2}$$

where H is an overall lengthscale, say the total height of the wall, and Gr is the Grashof number based on this length and ρ_1'; they take the form

$$\left.\begin{aligned} \psi &= \nu Gr^{\frac{1}{4}}\left(\frac{z}{H}\right)^{\frac{3}{4}}f(\eta) \\ \text{and}\qquad \gamma &= \rho'/\rho_1' = g(\eta). \end{aligned}\right\} \tag{7.4.3}$$

It is clear from the form of η that the thickness of the buoyant layer increases like $z^{\frac{1}{4}}$. Further, (7.4.3) shows that both the local Nusselt number and the integrated value (which compares the actual heat flux over the whole depth H with the purely conductive flux) are proportional to $(Gr)^{\frac{1}{4}}$. This is a general result for laminar flows, arising from the structure of the boundary layer equations (7.4.1), and it is applicable to other shapes provided only that the heated layer remains thin compared to the overall dimensions of the body.

The resulting ordinary differential equations, from which $f(\eta)$ and $g(\eta)$ are obtained, still contain an explicit dependence on κ and thus on Pr. Ostrach (1964) has calculated their forms numerically for a range of values of Pr. The dependence is complicated, but for values near that of air and greater, it is approximately $Pr^{\frac{1}{4}}$, so that $Nu \propto Ra^{\frac{1}{4}}$. The measured values of the flux, and the profiles predicted by these calculations, are in excellent agreement with laboratory measurements made in air.

The stability of these flows against a vertical plate has also been studied theoretically and experimentally. It is observed that turbulence sets in at overall Grashof number of about 10^9, corresponding to a boundary layer Reynolds number of a few hundred (see §4.2.3). It was first assumed that the stability criteria (for both the inviscid and viscous problems) are identical to those obtained for the same velocity profile in classical stability theory, the buoyancy forces just acting to produce this mean profile. It has been shown, however (see for example Gill and Davey (1969) and the review by Gebhart (1969)), that the inclusion of the buoyancy source of disturbance energy makes a substantial difference to the theoretical stability curves, lowering the critical Gr or Re and the wavenumber at which this is attained. These predictions, for the case of a plate in air through which a constant flux is maintained (a variation of the more usual condition of constant temperature), were confirmed by Polymeropoulos and Gebhart (1967). They created artificial disturbances of known frequency and amplitude using an oscillating ribbon, and watched the growth or decay of the waves, using an interferometer which gives contours whose separation is inversely proportional to the temperature gradient; two of their beautiful photographs are reproduced in fig. 7.19 pl. XVIII. More will be

said about this stability problem and its dependence on Prandtl number in §7.4.3.

7.4.2. *Buoyancy layers at vertical and sloping boundaries*

If the plane surface is not parallel to gravity but is at an angle θ to the horizontal, the equations describing the flow in an otherwise unconfined uniform environment remain the same except that $\sin\theta$ multiplies the body force term. The above solutions will therefore apply to the laminar case with $Gr\sin\theta$ replacing Gr in (7.4.2) and (7.4.3) (see also §4.2.3). This extension will of course be valid only when the flow is statically stable (for example when it is confined to the underside of a heated plate). On the upper surface of an inclined heated plate instability will set in much earlier. The observations of Lloyd and Sparrow (1970) show that for angles of inclination from the vertical greater than 14°, the wave-like instability illustrated in fig. 7.19 is replaced by longitudinal rolls (which is the preferred mode for Bénard convection in the presence of a shear). At higher Grashof numbers, the flow becomes more like the turbulent convection over a horizontal plate described in §7.2.2, with the addition of a mean flow up the plate (Tritton 1963).

When there is a stable density (temperature) gradient in the environment however, the heating of the upper surface of an inclined plate has quite a different effect, since the buoyant fluid now cannot rise indefinitely but remains confined to a layer near the boundary. A 'buoyancy layer' of this kind is important whenever the boundary conditions cannot match those imposed in the interior; it occurs at both vertical and sloping boundaries when there is a flux through the wall. Another, more surprising, result discussed below is that a sloping boundary through which there is *no* flux will also produce a flow near the wall in a stably stratified fluid. Gill (1966) and Veronis (1967) have pointed out that there is an exact analogy between this buoyancy layer, whose growth is limited by stratification, and the Ekman layer in a rotating fluid (see §9.2.4).

The laminar problem will first be considered, with the simple boundary conditions proposed by Prandtl (1952, p. 422) namely, a uniform gradient $G = N^2$ in the interior and a *fixed* density difference between the fluid near a sloping wall and that in the interior

at the same horizontal level. No position along the boundary is then distinguishable from any other, so one can expect solutions which depend only on the coordinate n normal to the slope and not on s parallel to it. Writing the differences from a standard density ρ_0 in the form

$$g\frac{\Delta\rho}{\rho_0} = Gz - g' \tag{7.4.4}$$

the equation of motion giving the velocity u parallel to the slope is

$$g'\sin\theta + \nu\frac{\partial^2 u}{\partial n^2} = 0. \tag{7.4.5}$$

The diffusion equation must include derivatives in the s-direction, but using (7.4.4) and the relation $z = s\sin\theta + n\cos\theta$ it can be reduced to

$$uG\sin\theta = \kappa\frac{\partial^2 g'}{\partial n^2}. \tag{7.4.6}$$

Either u or g' can be eliminated from (7.4.5) and (7.4.6) to give a single equation for the other variable. The solutions can be written as

$$\left.\begin{aligned} \rho' &= \rho_1'\,e^{-\xi}\cos\xi, \\ u &= g_1'\left(\frac{\kappa}{\nu G}\right)^{\frac{1}{2}} e^{-\xi}\sin\xi \end{aligned}\right\} \tag{7.4.7}$$

and these are shown in fig. 7.20. Here $\xi = n/l$, and the lengthscale l ('the thickness of the buoyancy layer') is given by

$$l^4 = 4\kappa\nu/G\sin^2\theta = 4\kappa\nu/N^2\sin^2\theta. \tag{7.4.8}$$

Notice that with these boundary conditions the maximum velocity is independent of the angle θ, though the normal distance from the boundary at which this is achieved does depend on θ through l. Prandtl has suggested an application to the phenomenon of 'mountain and valley winds', which blow down or up a valley when the slopes are cooled or heated.

Phillips (1970) and Wunsch (1970) have given solutions to the same equations with a stable linear gradient but with a boundary condition corresponding to no flux of solute through a solid sloping wall. This condition implies that the surfaces of constant density will be distorted so that they are normal to the slope as the slope is

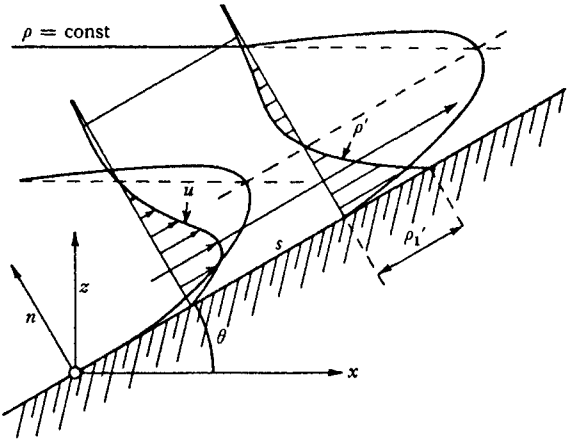

Fig. 7.20. The velocity, density and density anomaly profiles for a buoyancy layer in a linearly stratified environment, with the boundary condition of constant density difference. (From Prandtl (1952), reproduced by permission of Vieweg und Sohn.)

approached; the fluid against the wall will therefore be lighter than that in the interior at the same level and there will be an upslope current in a layer of depth l given by (7.4.8). Under laboratory conditions using dissolved salt this flow is very small (but detectable), though Phillips has shown that similar convective transports along narrow nearly horizontal slots could greatly exceed the purely diffusive vertical flux.

Prandtl has proposed a turbulent solution for the 'valley wind' problem, based on mixing length arguments which make κ and ν irrelevant. The velocity and depth are again constant, and by dimensional reasoning depend on g_1' and N through $u \propto g_1'/N$ and $l \propto g_1'/N^2$; the dependence on θ can be obtained by a more mechanistic argument. Such solutions can only remain valid when the entrainment is small. When turbulent mixing dominates (on steep slopes) then the depth will increase and be a function of slope (see §6.2); so too will the velocity when the buoyancy flux is changing. For example, a two-dimensional turbulent plume with a constant density difference between the plume and the environment just outside it will have $h \propto s$ and $u \propto s^{\frac{1}{2}}$.

7.4.3. *Convection in a slot*

An important example of a convective circulation in a totally enclosed region is that of fluid contained in a two-dimensional slot with vertical walls maintained at different temperatures. The flow is completely specified by three parameters, a Rayleigh number Ra_L based on the temperature difference and the width L, the Prandtl number, and the aspect ratio $h = H/L$, which can generally be taken as large so that the top and bottom boundaries have only a minor effect on the flow. We follow the description of Elder (1965*a*, *b*) who used a variety of laboratory techniques to obtain a clear picture of the flow at high Prandtl numbers in different ranges of Ra, and outline various theoretical analyses which have been suggested by the observations.

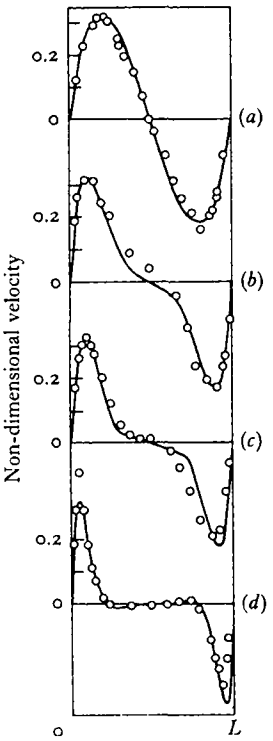

Fig. 7.21. Vertical velocity profiles in a slot at various Rayleigh numbers Ra_L; measurements compared with theory by Elder (1965*b*). (*a*) $Ra_L = 3.08 \times 10^4$, (*b*) 2.95×10^5, (*c*) 6.56×10^5, (*d*) 3.61×10^6.

For small $Ra_L (< 10^3)$ the temperature field is very close to that due to conduction alone, with a linear horizontal variation and no vertical temperature gradient. This horizontal density contrast will inevitably generate a slow steady circulation, up the hot wall and down the cold, but this makes a negligible contribution to the flux (except right at the top and bottom). As Ra_L increases, the isotherms become progressively more distorted, as shown in fig. 7.21. In the range $10^3 < Ra_L < 10^5$ large temperature gradients are established near the walls, with a uniform *stable* vertical gradient in the interior. (Compare with the mechanism discussed in §7.3.3.) There is a strong convective flow concentrated near the walls that transfers a larger fraction of the heat as Ra is increased. Above

$Ra_L = 10^5$ the interior region has superimposed on it a secondary flow consisting of a regular cellular pattern. The number of cells in the vertical increases with Ra, until at $Ra_L = 10^6$, when the amplitude of this secondary motion is large, counter-rotating cellular motions are generated in the weak shear regions between the larger cells.

The first theoretical discussions of the primary convective flow in the boundary layers (due to Pillow (1952) and Batchelor (1954*b*)) assumed that the interior region should have a constant temperature and a constant non-zero vorticity, which is not in accord with the observations described above. Many other experiments, such as those of Eckert and Carlson (1961) in air, now also support the view that the interior region has a stable stratification. Gill (1966) derived the 'buoyancy layer' solutions described above, and showed how it is possible to maintain boundary layers which are not entraining, but have constant velocity (7.4.7) and thickness (7.4.8). The vertical gradient G in Elder's experiments was approximately related to the overall temperature difference ΔT and height H by $G = \frac{1}{2}(g\Delta T/T_0)/H$, so that (7.4.8) becomes

$$l^4 \approx 8\kappa\nu H \Big/ \frac{g\Delta T}{T_0}. \tag{7.4.9}$$

Gill was able to go further, and include the boundary layer and interior in the same solution, which is shown in fig. 7.22. This allows for some entrainment in the lower part and outflow at the top of an upflowing layer, and its form is independent of Ra_L and H/L. The lengthscale l still determines the maximum thickness of the boundary layer, however, and the condition for this regime to be established is that l should be small compared with L. The solutions contain no disposable constant, the scaling being determined entirely by the boundary condition $w = 0$ at the top and bottom boundaries, and they are in good agreement with Elder's experimental results.

The stability of the laminar boundary layer regime on a vertical wall has been studied by Gill and Davey (1969), using numerical methods to cover the whole range of Prandtl numbers. They showed that the buoyancy-driven instability (as distinct from the purely mechanical instability arising from the shape of the velocity

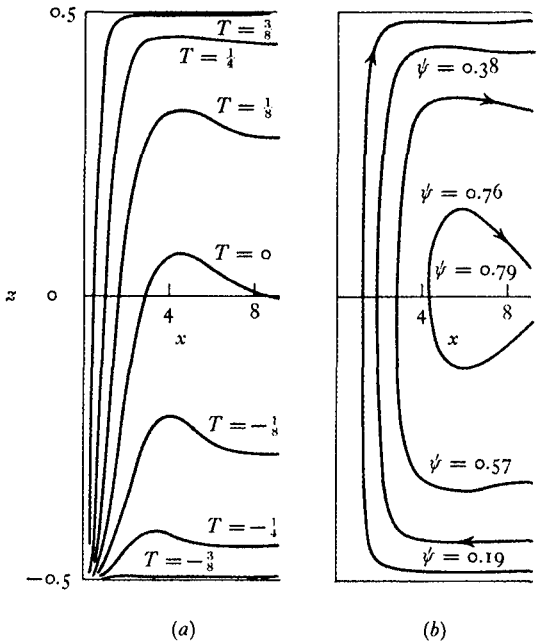

Fig. 7.22. (*a*) Isotherms and (*b*) streamlines for the boundary layer on the heated wall of a vertical slot. (From Gill 1966.)

profile) is increasingly important at large Pr, and that the Reynolds number for instability decreases with increasing Pr. Both diffusion and the stable gradient have an inhibiting effect on the growthrate of disturbances, which have the form of waves travelling faster than the flow. In the application to the slot, the critical condition is determined by a value of $Ra_L h^3$, i.e. a Rayleigh number Ra_H based of the vertical dimension (cf. §7.4.1), and varies strongly with Prandtl number.

In contrast, the breakdown of the conduction dominated flow (before strong boundary layers have formed) occurs in the form of stationary waves, and appears to be 'mechanically' driven. The critical value of Ra_L is independent of the aspect ratio h, but still depends on Pr. These results have an important application in the field of thermal insulation. The effectiveness of double walls or windows in minimizing the heat losses in air seems to depend on the stability of the conduction regime, rather than the change from

conduction to the boundary layer form of motion. Both instabilities are suppressed in a porous medium, and this is probably the main effect of filling a cavity with insulating foam.

The stability of the flow in a vertical slot when there is a vertical temperature gradient in either sense as well as a horizontal gradient has been investigated by Birikh, Gershuni and Zhukhovitshii (1969). Space does not allow us to discuss this here, but the reference quoted also gives a good introduction to earlier Russian work in this field. Much more could be said too about observations and theories dealing with related geometries; for example, Hart (1971*a*) has examined the convective motions (and their stability) in a tilted narrow slot, and Walin (1971) has considered the relation between the boundary layer flows and the stratification in a closed region of any shape. Convection in a region of variable depth will be considered in the more specialized context of the next chapter (§8.3.4), though some of the results are valid regardless of how the buoyancy flux is supplied.

Finally, let us consider the experimental results of Elder (1965*b*) for unsteady and turbulent flows in a slot. Using water as the working fluid, he observed travelling wave-like motions at the edge of the boundary layers (cf. fig. 7.19), which appeared at $Ra_H \sim 10^9$, much as they do at a single wall. At higher values of Ra_H the waves grow and break, and there is an intense interaction between the wall layer and the interior, both of which become turbulent. This strongly turbulent flow, in which the mean temperature is nearly constant and the mean velocity zero across the interior region, can be used to test some of the predictions of the theories of thermal turbulence. For example the horizontal temperature profile has a conduction region with linear temperature gradient (presumably in a marginally stable state, similar to that discussed in §7.3.1), a substantial region where the temperature varies with $z^{-\frac{1}{3}}$ and finally the uniform interior. The existence of the $z^{-\frac{1}{3}}$ region, which did not appear in Townsend's (1959) experiments on a horizontal surface but which is characteristic of free convection profiles in the atmosphere (§5.1.3), is at first sight surprising. As Elder pointed out however, the dimensional arguments leading to (5.1.15) require only that there should be a constant heat flux normal to the boundary, that the motion be driven entirely by buoyancy forces, and that molecular

processes be unimportant. All of these are satisfied in the intermediate mixing region, and the angle between the direction of gravity and the heat flux is irrelevant except for the evaluation of the numerical factor. The total heat transport between tall vertical plates in the turbulent range can be expressed (Jakob 1957) as $Nu = 0.053\, Ra_L^{\frac{1}{3}}$, so the multiplying constant is rather smaller than it is for horizontal plates.